Stable Realization of a Delay System Modeling a Convergent Acoustic Cone

Rémi Mignot, Thomas Hélie, and Denis Matignon

Abstract— **This paper deals with the physical modeling and the digital time simulation of acoustic pipes. We will study the simplified case of a single *convergent* cone. It is modeled by a linear system made of delays and a transfer function which represents the wave reflection at the entry of the cone.**

According to [1], the input/output relation of this system is causal and stable whereas the reflection function is *unstable*.

In the continuous time-domain, a first state space representation of this delay system is done. Then, we use a change of state to separate the unobservable subspace and its orthogonal complement, which is observable. Whereas the unobservable part is unstable, it is proved that the observable part is stable, using the *D-Subdivision* method. Thus, isolating this latter observable subspace, to build the minimal realization, defines a stable system. Finally, a discrete-time version of this system is derived and is proved to be stable using the *Jury criterion*.

The main contribution of this work is neither the minimal realization of the system nor the proofs of stability, but it is rather the solving of an old problem of *acoustics* which has been achieved using standard tools of *automatic control*.

I. INTRODUCTION

We are interested in the physical modeling of wind instruments in order to perform the digital time simulation of the acoustic behavior of the resonator. We use the digital waveguides approach (cf. [2]), which is well adapted for sound synthesis. In two references (cf. [3], [4]), it has been proposed to concatenate elementary conical pipes, in order to build the complete tube with a refined approximation of the tube radius. Wave propagations are modeled by a pure delay operator (with or without damping), and the wave reflections at junctions of cones are modeled by first-order transfer functions.

Unfortunately, if the slope difference between two adjoining cones is negative, a problem occurs: although the wave propagation and the physics is conservative (and thus input/output relations for a piece of pipe define stable systems), the reflection at the junction is unstable and cannot yield, at least straightforwardly, stable numerical simulations.

In [1], this paradox is explained for a single *convergent* cone and a calculation method is proposed. But, this solution is not satisfactory for numerical simulation in time domain on an infinite time range. In [3], a simulation which proves to be stable in practice is proposed. But, the stability of the digital system is only "qualitatively justified" (because of the physical stability of the modeled system) and no proof is given. In [4], the digital time-simulation is performed using a numerical convolution by the impulse response of the global reflection of pieces of pipe. Because the global reflection is stable, this method ensures the stability for digital simulation on an infinite horizon. But the CPU cost is so high that it prevents real-time simulation.

In this paper, we consider the simplified case of the convergent cones as in [1], we derive a low-cost simulation which reveals to be similar to that of [3], and we prove stability.

The paper is organized as follows: in section II, we present the truncated convergent cone, and according to the acoustic equations, we give the analytical expressions of the transfer function in the Laplace domain. In section III, we build a state space representation of this system, and we show that the unobservable subpart is unstable. Then we derive the minimal realization with its orthogonal complementary subspace which corresponds to an observable substate. Section IV gives the proof of the stability of this observable substate, using the D-Subdivision method. Section V briefly presents the discrete-time approximation of the minimal realization and gives outlines of the proof of stability of this digital system, using the Jury criterion. In section VI, we discuss future works for the stability proof of concatenation of several conical pieces of pipe.

II. ACOUSTIC MODEL OF A SINGLE CONE

A. Acoustics Equations

In lossless conical pipes, the acoustic pressure p and the particular velocity v are characterized by the *horn equation* (cf. [5], [4]) and Euler equation:

$$\left(\frac{\partial^2}{\partial x^2}-\frac{1}{c_0^2}\frac{\partial^2}{\partial t^2}\right)(p(x,t)) = -2\frac{r'(x)}{r(x)}\frac{\partial}{\partial x}p(x,t), \quad (1)$$

$$\rho_0\frac{\partial}{\partial t}v(x,t)+\frac{\partial}{\partial x}p(x,t) = 0. \quad (2)$$

In this one-dimensional acoustic model, x is the axis coordinate of the cone, r is the radius, $c_0 = 340 m.\mathrm{s}^{-1}$ is the speed of sound and $\rho_0 = 1.2 kg.m^{-3}$ is the mass density.

B. Traveling Waves

Let $\phi^+(x,t)$ and $\phi^-(x,t)$ be defined by:

$$\begin{bmatrix}\phi^+(x,t)\\ \phi^-(x,t)\end{bmatrix} := \frac{r(x)}{2}\begin{bmatrix}1 & \rho_0 c_0\\ 1 & -\rho_0 c_0\end{bmatrix}\begin{bmatrix}p(x,t)\\ v(x,t)\end{bmatrix}. \quad (3)$$

This work is supported by the CONSONNES project, ANR-05-BLAN-0097-01

Rémi Mignot and Thomas Hélie are with IRCAM & CNRS, UMR 9912, 1, place Igor Stravinsky, 75004 Paris, France {mignot,helie}@ircam.fr

D. Matignon is with University of Toulouse; Institut Supérieur de l'Aéronautique et de l'Espace, Applied Mathematics training unit; 10, av. E. Belin 31055 Toulouse Cedex 4, France. denis.matignon@isae.fr

Rémi Mignot is a Ph.D. student at Télécom Paris/TSI.

For planar waves traveling inside a lossless bore, the acoustic state $\phi^{\pm}$ corresponds to the standard decoupled progressive planar waves. Inside conical bore, these waves are still progressive so that they preserve the causality principle.

C. Junction of Pipes

At the junction of a cylinder and a cone, the traveling waves are partially reflected in the opposite direction and are partially transmitted to the other side of the junction. In this work, we only consider junction with section continuity.

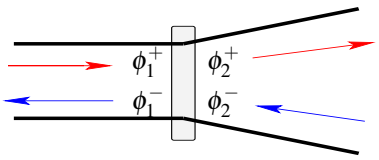

Fig. 1. Junction of a cylinder and a cone

With the pressure and the flow continuity on both sides, we get the analytical expressions of the reflections and transmissions at junctions (cf. [4]), which leads to the following scattering matrix in the Laplace domain:

$$\begin{bmatrix} \phi_1^-(s) \\ \phi_2^+(s) \end{bmatrix} = \begin{bmatrix} R(s) & 1+R(s) \\ 1+R(s) & R(s) \end{bmatrix} \begin{bmatrix} \phi_1^+(s) \\ \phi_2^-(s) \end{bmatrix}, \tag{4}$$

$$\text{with } R(s) = \frac{\alpha}{s-\alpha}, \tag{5}$$

where $\alpha := -\frac{c_0}{2}\frac{r'}{r_j}$, r' is the slope of the cone, r_j is the radius at the junction and s is the Laplace variable.

In the case of a convergent cone, $r' < 0$, α is positive and the junction reflection $R(s)$ is unstable.

D. Case of a Truncated Convergent Cone

To simplify the study, consider a simple case where a truncated convergent cone of length L is connected to a cylinder and is terminated by a zero impedance, as Fig. 2 shows. In [1] the same case is presented (with different notations).

The progressive waves are decoupled, the traveling effect is modeled by a pure delay operator $\mathrm{e}^{-\tau s}$, where $\tau = L/c_0$, and the zero impedance corresponds to a reflection coefficient which is -1. Figure 3 represents the structure of the system.

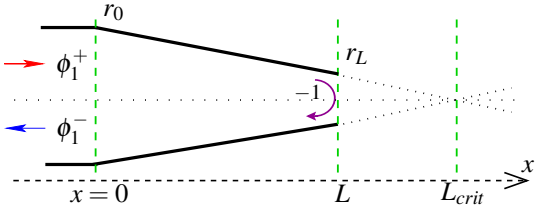

Fig. 2. Truncated convergent cone

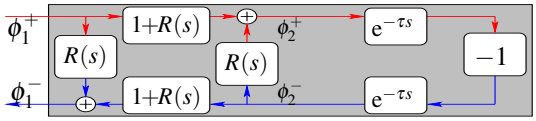

Fig. 3. Structure of the truncated convergent cone

The calculation of the *global* reflection, $R_g(s)$, of the system gives the following analytical expressions:

$$\begin{aligned} R_g(s) &:= \frac{\phi_1^-(s)}{\phi_1^+(s)} = R(s) - \frac{\big(1+R(s)\big)^2 \mathrm{e}^{-2\tau s}}{1+R(s)\,\mathrm{e}^{-2\tau s}} \\ &= \frac{\alpha - (s+\alpha)\,\mathrm{e}^{-Ts}}{s-\alpha+\alpha\,\mathrm{e}^{-Ts}}. \end{aligned} \tag{6}$$

where $T := 2\tau$. We define L_{crit} the length for which the radius of the right end is zero, $r(L_{crit}) = 0$. It is given by $L_{crit} = -r_0/r' = c_0/(2\alpha)$, as $r' = (r_L - r_0)/L$.

Whereas the junction reflection $R(s)$ is unstable, numerical study reveals that the *global* reflection $R_g(s)$ is stable with $L < L_{crit}$. This **paradox** is well-known and has been explained in [1]. The transfer function $R(s)$ represents the reflection due to the slope discontinuity at the junction of two anechoic tubes. However, a convergent cone cannot be physically anechoic, and the stability, or the causality, cannot be ensured. Nevertheless, the successive forward and backward waves propagations through the truncated cone stabilize the *global* reflection of the system.

In spite of the input/output stability, for the simulation of the system, it is absolutely necessary to study the stability of the relations between the input and the substates.

E. Adimensional Problem

Now we define the following adimensional problem:

Original variable (unit)	T (s)	s (s^{-1})	α (s^{-1})
Adimensional variable	$\underline{T} := 1$	$\underline{s} := sT$	$\xi := \alpha T$

and we define the adimensional version of every function X by $\underline{X}(\underline{s}) := X(\underline{s}/T)$.

Remarks: Firstly, we can notice that the case $\xi = 1$ corresponds to the critical case where $T = T_{crit} := 2L_{crit}/c_0$. Secondly, the expressions of $\underline{R}(\underline{s})$ and $\underline{R}_g(\underline{s})$ depend only on one coefficient ξ. This shows that stability results will be expressed in terms of $\alpha T = \xi$ only.

The change of variable $\underline{s} = sT$ preserves the Laplace domain of stability ($\Re\mathrm{e}(\underline{s}) > 0 \Leftrightarrow \Re\mathrm{e}(s) > 0$), since $T > 0$.

To simplify notations, except notification, $\underline{s}$ is renoted s in the following.

III. State-Space Representation and Minimal Realisation

A. Equations of the System

In the adimensional version of equation (4), let's replace the notation $\underline{\phi}_1^+$, $\underline{\phi}_1^-$, $\underline{\phi}_2^+$ and $\underline{\phi}_2^-$ by respectively: u, y, e_1 and e_2. Where u is the input of the system and y is the output. Equation (4) of the junction becomes:

$$\begin{cases} y &= \underline{R}(s)u + \underline{R}(s)e_2 + e_2, \\ e_1 &= \underline{R}(s)u + \underline{R}(s)e_2 + u, \end{cases}$$

with $\underline{R}(s) = \xi/(s-\xi)$. Defining the substates of the system x_1 and x_2 as $x_1 := \underline{R}(s)\,u$ and $x_2 := \underline{R}(s)\,e_2$, and replacing e_2 by $e_2 = -\mathrm{e}^{-s}\,e_1$, we get the following representation of the system:

$$\left\{\begin{array}{rcl} sX(s) &=& A(s)X(s)+B(s)u(s),\\ y(s) &=& C(s)X(s)+D(s)u(s),\end{array}\right. \tag{7}$$

with $X=[x_1,x_2]^{\mathrm{T}}$ is the state vector. A,B,C and D correspond to linear operators, they are given by the following matrices:

$$A(s) = \begin{bmatrix} \xi & 0 \\ -\xi\,\mathrm{e}^{-s} & \xi(1-\mathrm{e}^{-s})\end{bmatrix}, \tag{8}$$

$$B(s) = \begin{bmatrix} \xi \\ -\xi\,\mathrm{e}^{-s}\end{bmatrix}, \tag{9}$$

$$C(s) = \begin{bmatrix} 1-\mathrm{e}^{-s} & 1-\mathrm{e}^{-s}\end{bmatrix}, \tag{10}$$

$$D(s) = -\mathrm{e}^{-s}. \tag{11}$$

Thus (7) is a state-space representation of a linear delay-differential system. In order to study the stability of all internal variables of the system, outputs and substates, we must study the eigen-values of the matrix $A(s)$ which are the roots of the characteristic function:

$$\det\big(sI_2 - A(s)\big) = \big(s-\xi\big)\big(s-\xi+\xi\,\mathrm{e}^{-s}\big). \tag{12}$$

In the case of convergent cones, $\xi>0$, the matrix $A(s)$ has at least one positive eigen-value, and the input/state relation is not stable. In a first step, it is necessary to rewrite the system in order to isolate this instability.

B. Kalman's Form

By studying the observability of the previous system, we notice that the dimension of the unobservable subspace is 1. So, because we are only interested in the input/output relation, it is possible to reduce the dimension of the system by isolating the unobservable subspace. We define the following change of variables:

$$Z = \begin{bmatrix} z_1 \\ z_2\end{bmatrix} = QX = \frac{1}{2}\begin{bmatrix} 1 & 1 \\ 1 & -1\end{bmatrix}\begin{bmatrix} x_1 \\ x_2\end{bmatrix}, \tag{13}$$

thus the dynamic matrix and the observation matrix become:

$$A^z(s) = \begin{bmatrix} \xi(1-\mathrm{e}^{-s}) & 0 \\ \xi\,\mathrm{e}^{-s} & \xi\end{bmatrix}, \tag{14}$$

$$C^z(s) = \begin{bmatrix} 1-\mathrm{e}^{-s} & 0\end{bmatrix}. \tag{15}$$

This form of the system is the canonical form for the observability, which is here the Kalman's form (cf. [6]). We notice that z_1 is decoupled from z_2, and the latter does not affect the output. z_1 is an observable substate and z_2 is an unobservable substate. So it is not necessary to simulate z_2, because only z_1 acts on the output.

C. Minimal Realization

Eliminating the substate z_2, we get the *minimal realization* which leads to:

$$\left\{\begin{array}{rcl} s\,z_1(s) &=& \xi\,(1-\mathrm{e}^{-s})\,z_1(s)+\xi\,(1-\mathrm{e}^{-s})\,u(s),\\ y(s) &=& (1-\mathrm{e}^{-s})\,z_1(s) \;-\; \mathrm{e}^{-s}\,u(s).\end{array}\right. \tag{16}$$

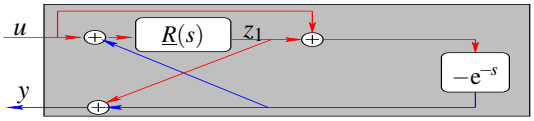

Fig. 4. Structure of the minimal realization

This system corresponds to the structure in Fig.4, where $\underline{R}(s) = \xi/(s-\xi)$. We notice that the minimal realization corresponds to the so-called *Kelly-Lochbaum* structure which is very efficient and used in waveguide simulations (cf. [7]).

Remark: This result is not new and the system (7) seems naive and artificial, but the reasoning explained here, is interesting in the case of more complex acoustic models as discussed in conclusion.

The characteristic equation of this system is:

$$d(s) := s-\xi+\xi\,\mathrm{e}^{-s} = 0. \tag{17}$$

From this system, we define two transfer functions:

$$\underline{F}(s) := \frac{z_1(s)}{u(s)} = \frac{\xi\big(1-\mathrm{e}^{-s}\big)}{s-\xi+\xi\,\mathrm{e}^{-s}}, \tag{18}$$

$$\underline{R}_g(s) := \frac{y(s)}{u(s)} = \frac{\xi-\big(s+\xi\big)\,\mathrm{e}^{-s}}{s-\xi+\xi\,\mathrm{e}^{-s}}. \tag{19}$$

We notice that this reduction has removed an unstable root because the factor $(s-\xi)$ has disappeared. Now we must study the roots of the characteristic equation (17), (which include the poles of the two previous transfer functions).

IV. Stability Study in Continuous Time

A. Numerical Observations and Interpretation

Numerically, we noticed that all roots of the characteristic equation, $d(s)=0$ (cf. (17)), are stable (negative real part), except one, which is stable when $\xi<1$ but which becomes unstable when $\xi>1$.

According to this observation, the upper boundary of ξ which ensures the system stability, is $\xi=1$. It corresponds to the critical length, L_{crit}, for which the radius of the convergent cone is zero (and becomes negative beyond L_{crit}). Thus a pipe with $L>L_{crit}$ is physically unrealizable, and the stability cannot be guaranteed by a physical validation.

The whole section is devoted to prove what we have brought to light by a numerical way.

B. D-Subdivision Method

To study the stability of the system, we have to determine the position of the roots of the characteristic function with respect to the imaginary axis. But it is not necessary to express them analytically, we just have to check how many roots have positive real part. The *D-Subdivision* method makes such an analysis possible (cf. [8], [9]).

Consider a general system characterized by a characteristic polynomial of the dependent variables $s\in\mathbb{C}$ and e^{-s}, with real coefficients $\{a_j\}$. Since the roots position moves continuously when the values of parameters vary continuously, the number of unstable roots changes when one or several roots appear on the imaginary axis. So it is possible to divide the

space of parameters $\{a_j\}$ into *domains* in which the number of unstable roots is constant. Their *boundaries* are thus given, for one fixed T, by:

$$\Big\{a_j \in \mathbb{R}/\exists \omega \in \mathbb{R}, d(i\omega) = 0\Big\}. \tag{20}$$

Using the *D-Subdivision* method we prove the following

Theorem: **Characteristic equation (17) has no root with strictly positive real part when $\xi < 1$.** That is,

$$\forall \xi < 1 \text{ and } \forall s \in \mathbb{C}/\Re\mathrm{e}(s) > 0, \quad d(s) = s - \xi + \xi\, \mathrm{e}^{-s} \neq 0.$$

C. Proof

Let's define the following function:

$$G_{\beta,\gamma}(s) := s - \beta + \gamma \mathrm{e}^{-s}. \tag{21}$$

For educational purposes, it is interesting to duplicate the coefficient ξ into (β,γ); it allows to represent every root.

To know the stability *domain* of the function $G_{\beta,\gamma}(s)$ we have to determine the *boundaries* of *domains* in the β,γ-*plane*. That is obtain a characterization of all the solutions of "$\exists \omega \in \mathbb{R}/G_{\beta,\gamma}(i\omega) = 0$" in function of β and γ.

A first obvious *boundary* is given by $\beta = \gamma$. It corresponds to a single root at $s = 0$. Using the case where $\gamma = 0$ and $\beta < 0$, we can verify that this root is on the left side of the imaginary axis for $\gamma < \beta$ and goes to the right side for $\gamma > \beta$. This *boundary* is represented by curve (b1) in Fig. 5.

The other *boundaries* are given by solving $G_{\beta,\gamma}(i\omega) = 0$ with respect to ω:

$$G_{\beta,\gamma}(i\omega) := i\omega + \beta - \gamma\big(\cos(\omega) - i\sin(\omega)\big) = 0,$$

$$\Leftrightarrow \left\{ \begin{array}{rcl} \beta - \gamma\cos(\omega) & = & 0, \\ \omega - \gamma\sin(\omega) & = & 0. \end{array} \right. \tag{22}$$

This gives the *boundaries* curves, parametrized by $\omega \in \mathbb{R}$:

$$\left\{ \begin{array}{rcl} \beta(\omega) & = & \omega\cot(\omega), \\ \gamma(\omega) & = & \omega/\sin(\omega). \end{array} \right. \tag{23}$$

$\beta(\omega)$ and $\gamma(\omega)$ are even functions, these curves are identically described once for $\omega \in \mathbb{R}^-$ and once for $\omega \in \mathbb{R}^+$. They correspond to the passing of two complex conjugate roots through the imaginary axis, $-i\omega$ and $i\omega$. Figure 5 shows the *boundaries* and the number P of unstable roots in each *domain*. Curve (b2) represents the first boundary $(\omega \in]-\pi,\pi[)$.

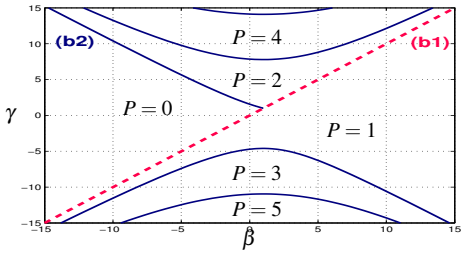

Fig. 5. Domains of Subdivision.

Since $d(s) = G_{\xi,\xi}(s)$, our particular case is on boundary (b1) (i.e. $\xi = \beta = \gamma$), and so it is at the limit of the stability because there is a single root at $s = 0$.

This line crosses boundary (b2) at the point $(\beta(0),\gamma(0)) = (1,1)$, another root which is stable when $\beta = \gamma < 1$ becomes unstable when $\beta = \gamma > 1$. Thus, with $\beta = \gamma = \xi$, the condition of stability of the convergent cone is $\xi < 1$.

Consequently, the characteristic function $d(s)$ has a *single* root at $s = 0$ for all ξ, infinitely many stable roots, and one root which is stable when $\xi < 1$ and unstable when $\xi > 1$.

Remark: Because of the single root at $s = 0$, the system under study is at the limit of stability. Nonetheless, the Taylor series expansions of the functions $\underline{R_g}$ et $\underline{F}$ (cf. (18)- (19)) at this point are: $\underline{R_g}(s) = -1 + O(s)$ and $\underline{F}(s) = \xi/(1-\xi) + O(s)$, when $s \sim 0$. It means that this root, which behaves as a pure integrator, is compensated with numerators of $\underline{R_g}$ and $\underline{F}$.

V. STABLE SIMULATION IN DISCRETE TIME

A. Derivation of a Digital Simulation

In this section, we use the dimensional variables (cf. section II-E).

For numerical simulations, we must discretize the system. As (7) (and Fig. 3) involves unstable states, it is hopeless to derive a stable digital version. It is the reason why we choose to get a discrete-time system from (16) (and Fig. 4).

For low-cost simulations, we discretize e^{-sT} and $R(s)$ separately. If $T = NT_e$ (where T_e is the sampling period and $N \in \mathbb{N}$) the operator e^{-sT} becomes Z^{-N} in the *Z-Transform* domain, which is simulated by an economical circular buffer.

About the discretization of $R(s)$ to its digital version $R^d(Z)$, even if the chosen method conserves the stability properties of $R(s)$, the digital version of the global system (with loop) may become unstable. For example, numerical simulations reveal that using the standard *bilinear transform* (cf. [10]) makes the system unstable for some α and T.

Here, we propose to use the *triangle approximation* (modified first-order hold cf. [11]) given by

$$R(s) = \frac{\alpha}{s - \alpha} \quad \Rightarrow \quad R^d(Z) = \frac{b_0 Z + b_1}{Z - a},$$

with $a = \mathrm{e}^{\alpha T_e}$, $b_0 = -\frac{1-a}{\alpha T_e} - 1$ and $b_1 = \frac{1-a}{\alpha T_e} + a$. This method leads to a stable digital system as detailed in next section.

Calculating the dynamic equation of the discrete-time system, we obtain the following characteristic polynomial:

$$P(Z) := Z^{N+1} - aZ^N + b_0 Z + b_1 = \sum_{i=0}^{N+1} p_i Z^{N+1-i}. \tag{24}$$

In order to study stability, we have to know if at least one root has its modulus higher than 1. We propose to use Jury criterion to prove the stability of this discrete-time system.

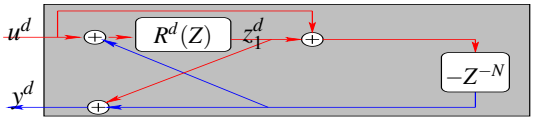

Fig. 6. Structure of the digital system

B. Jury Criterion

Here, we give the *Jury criterion* (cf. [12]). Considering the polynomial $P(Z)=\sum_{j=0}^{N+1} p_j Z^{N+1-j}$, with $p_0=1>0$, *Jury criterion* proves that it has no complex root outside the unity circle if and only if all the following assumptions are verified:

C1: $P(Z=1)>0$,
C2: $(-1)^{N+1}P(Z=-1)>0$,
C3: $p_0 > \mid p_{N+1} \mid$,
C4: Defining the following inductive relation:

$$\begin{cases} p_{(k+1,j)} := p_{(k,0)}p_{(k,j)} - p_{(k,N+1-k)}p_{(k,N+1-k-j)}, \\ \forall k \in [0,N-2]_{\mathbb{N}} \text{ and } \forall j \in [0,N-k]_{\mathbb{N}}, \end{cases}$$

with $p_{(0,j)} := p_j$, $\forall j \in [0,N+1]_{\mathbb{N}}$, last assumptions are:

$$p_{(k,0)} > \left| p_{(k,N+1-k)} \right|, \quad \forall k \in [1,N-1]_{\mathbb{N}}.$$

Next, we present the outlines of the proof of the stability using the *Jury criterion*. Assumption (C1) needs a few precisions, that's why we will deal with it at the end.

C. Proof Outlines

(C2): Separating the cases $\alpha>0$, $\alpha<0$, $\alpha=0$, we prove that (C2) is verified for all real α.

(C3): The case $\alpha=0$ is straightforward. Otherwise since $p_0=1$, we study the sign of $B(Y)=1-p_{N+1}$ with $Y=1-\alpha T_e$ for Y in $]0,1[$ and $]1,\infty[$. (C3) is verified if $\alpha T_e<1$.

(C4): This proof seems difficult, but the characteristic polynomial $P(Z)$ is sparse (cf. (24)), and it implies $p_{(k,j)}=0$ $\forall k \in [1,N-1]_{\mathbb{N}}$ and $\forall j \in [2,N-k]_{\mathbb{N}}$. Then, we can simplify the inductive relation as follows:

$$\begin{cases} f_{k+1} & := p_{(k+1,0)} & = & {f_k}^2 - {h_k}^2, \\ g_{k+1} & := p_{(k+1,1)} & = & f_k\, g_k, \\ h_{k+1} & := p_{(k+1,N-k)} & = & -h_k\, g_k. \end{cases} \tag{25}$$

We have succeeded to prove that the upper boundary of T is $T_{crit}=1/\alpha$ (cf. appendix). That means if $\alpha T<1$:

$$p_{(k,0)} > \left| p_{(k,N+1-k)} \right|, \quad \forall k \leq N-1.$$

(C1): The first assumption is not verified because $P(Z=1)=0$. However, that means the characteristic polynomial has a root at $Z=1$, thus the system has a pure integrator and it is at the limit of stability. Nonetheless we notice that, like with the continuous time system, the numerators of the two digital transfer functions which are equivalent to $F(s)$ and $R_g(s)$ (cf. (18) and (19)) are 0 at $Z=1$. As a result, the pure integrator is theoretically compensated.

Strictly speaking, the rigorous proof should be carried out on the polynomial Q such as $P(Z)=(Z-1)Q(Z)$. This has also been checked.

In conclusion, according to the discretization we have chosen, we reach the same result as in continuous time, that is the system is stable with $\xi=\alpha T<1$ and the pure integrator is theoretically compensated with the loop.

D. Digital Simulation

We have programmed in C-language the digital simulation of the system shown in Fig. 6, in order to check the previous results in practice.

Figure 7 shows the impulse response of the system, that is the output y_n^d when the input u_n^d is an impulse at $n=0$. The sampling frequency is $1/Te=44100Hz$, the delay value is $T=0.1s$ and $\alpha=9.99$ (this gives $a\simeq 1.000226$ and $N=4410$). We have chosen α and T such as $\alpha T<1$ and $\alpha>0$.

This graph reveals that the impulse response grows exponentially in the range $[0,T[$, and then the successive returns of the delay line compensate for this instability. A longer simulation shows that the simulated system is globally stable.

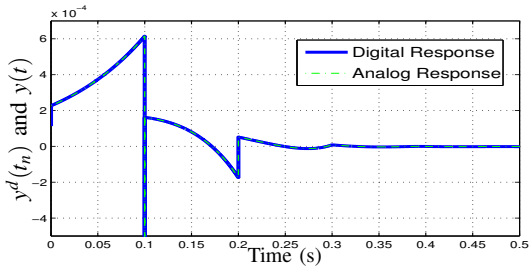

Fig. 7. Impulse response (with $T=0.1s$ and $\alpha=9.99\text{s}^{-1}$)

The comparison of Fig. 7 between the computed digital response and the analog response (given analytically in [1]) shows that they are very close. The relative mean error is less than 1 percent in the range $t\in[0,0.5]$.

Because of assumption (C1), in section V-C we have noticed a pole at $Z=1$ which may behave like a pure integrator, but which is theoretically compensated. For digital simulations, we had anticipated that the numerical approximation due to the truncation could produce an instability, fortunately computations revealed that the step response remains stable in practice.

VI. CONCLUSIONS AND FUTURE WORKS

A. Conclusions

In this paper, we have studied a 1D-model of propagation in a truncated convergent acoustic cone. Solving the equations leads to a simulation structure which includes a delay and the transfer function of an unstable system. The analysis of this structure reveals the system is input/output stable, whereas the internal state cannot be stabilized. As a consequence, this structure cannot be used to simulate the system.

To cope with this problem, a change of variables is performed and a Kalman's form is derived. While the unobservable subspace corresponds to an unstable part of the system, we prove that its orthogonal complement corresponds to a stable part. Then, isolating this observable part yields to a minimal realization, which both reduces the cost of simulation and defines a stable realization.

Thus, this paper illustrates how a tool of control engineering has helped to solve a well-known problem of acoustics with guaranteed stability and fully proved results.

B. Future Works

In order to simulate the model of a complete acoustic resonator of a wind instrument, we have to study the concatenation of cones, as it is done in [3], and in future works, we have to prove the stability of the whole structure.

With a refined acoustic model of lossy pipes with varying cross section (cf. [13], [14]), we have to study linear fractional differential systems with delay. But we are confronted with very similar problems of stability, with a higher level of complexity.

Even if the derived structure (cf. Fig. 4) is not new, the noticeable conclusion of this paper is the understanding of the instability. In the first system (cf. (7)), only the observable part is needed to describe the acoustic behavior. The unobservable part, which is unstable, is not justified physically. It has been introduced by the theoretical model, but has to be removed for simulation. We hope that what we have understood in this paper will help us to also derive stable realizations in the more complex case of lossy pipes with varying cross section.

APPENDIX

We define the following inductive relation:

$$\left\{\begin{array}{lcl} f_{k+1} & := & {f_k}^2 - {h_k}^2, \quad \forall k>0, \\ g_{k+1} & := & f_k\, g_k, \\ h_{k+1} & := & -h_k\, g_k, \end{array}\right. \tag{26}$$

with the initialisation:

$$\left\{\begin{array}{lcll} f_1 & := & 1-{b_0}^2 & = {p_0}^2 - {p_{N+1}}^2, \\ g_1 & := & -a-b_0\, b_1 & = p_0\, p_1 - p_{N+1}\, p_N, \\ h_1 & := & b_0 + a\, b_1 & = p_0\, p_N - p_{N+1}\, p_1, \end{array}\right.$$

and for $X := \alpha T_e$:

$$\left\{\begin{array}{lcll} a(X) & = & \mathrm{e}^X, & \forall X \in \mathbb{R}, \\ b_0(X) & = & -\left(\frac{1-\mathrm{e}^X}{X}\right) - 1, & \forall X \in \mathbb{R}^*, \\ b_1(X) & = & \left(\frac{1-\mathrm{e}^X}{X}\right) + \mathrm{e}^X, & \forall X \in \mathbb{R}^*. \end{array}\right.$$

To ensure continuity: $b_1(0) = b_0(0) = 0$.

Lemma: For all $k>0$ and X in $\left]-\infty, \frac{1}{k+1}\right[$, f_k and h_k defined by (26) verify:

$$f_k(X) > |h_k(X)|\,. \tag{27}$$

► With $X=0$, the proof is straightforward, but with $X \neq 0$ we have to define:

$$\eta_k(X) := \frac{f_k(X)}{h_k(X)}, \tag{28}$$

$\forall k>0$ and $\forall X \in \chi_k := \{X \in \mathbb{R} \,/\, f_k(X)\, h_k(X) \neq 0\}$.

In first time, by developing the expressions of h_k and h_{k+1}, we obtain the following relations $\forall k>1$ and $\forall X \in \chi_{k+1} \cap \chi_k \cap \chi_{k-1}$:

$$h_{k+1}(X) = h_k(X)^2\, \eta_{k-1}(X), \tag{29}$$

$$\eta_{k+1}(X) = \frac{1}{\eta_k(X)}\Big(\eta_{k-1}(X)^2 - 1\Big). \tag{30}$$

Using the definition of f_{k+1} (cf. (26)), (29) and (30), we prove by induction that $\forall k>0$:

- $$\left\{\begin{array}{lll} f_k(X) & >0, & \forall X \in \left]-\infty, \frac{1}{k}\right[, \\ h_k(X) & <0, & \forall X<0, \\ & >0, & \forall X \in \left]0, \frac{1}{k}\right[, \end{array}\right. \tag{31}$$
  and thus $\chi_k \supset \left]-\infty, \frac{1}{k}\right[\setminus \{0\}$.
- $$\eta_k(X) = \frac{1-kX}{X}, \quad \forall X \in \left]-\infty, \frac{1}{k}\right[\setminus \{0\}. \tag{32}$$
- Equation (32) implies (27) $\forall X \in \left]-\infty, \frac{1}{k+1}\right[\setminus \{0\}$. ◄

Finally, since $f_k = p_{(k,0)}$ and $h_k = p_{(k,N+1-k)}$ $\forall k \in [1, N-1]_{\mathbb{N}}$ (cf. (25)), (27) is equivalent to:

$$p_{(k,0)} > \left|p_{(k,N+1-k)}\right|, \ \forall X < \tfrac{1}{k+1}. \tag{33}$$

However, $\frac{1}{N} \leq \frac{1}{k+1}$, $X = \alpha T_e$ and $T = N T_e$, as a result if $\alpha T < 1$, the assumption (C4) is verified:

$$p_{(k,0)} > \left|p_{(k,N+1-k)}\right|, \ \forall k \in [1, N-1]_{\mathbb{N}}.$$

REFERENCES

[1] J. Gilbert, J. Kergomard, and J. D. Polack. On the reflection functions associated with discontinuities in conical bores. *J. Acoust. Soc. Am.*, 04, 1990.

[2] J. O. Smith. Physical modeling synthesis update. *Computer Music Journal*, 20(2):44–56, 1996. MIT Press.

[3] V. Välimäki. *Discrete-time modeling of acoustic tubes using fractional delay filters*. PhD thesis, Helsinski University of Technology, 1995.

[4] E. Ducasse. An alternative to the traveling-wave approach for use in two-port descriptions of acoustic bores. *J. Acoust. Soc. Am.*, 112:3031–3041, 2002.

[5] A. Webster. Acoustic impedance and the theory of horns and of the phonograph. *Proc. Nat. Acad. Sci. U.S*, 5, 1919.

[6] R. Kalman. Canonical structure of linear dynamical systems. In *Proceedings of the National Academy of Sciences*, pages 596–600, 1961.

[7] J. D. Markel and A. H. Gray. On autocorrelation equations as applied to speech analysis. *IEEE Trans. Audio and Electroacoust.*, AU-21(2):pp. 69–79, Apr 1973.

[8] V. B. Kolmanovskii and V. R. Nosov. *Stability of Functional Differential Equations*. Academic press, New York, 1986.

[9] S. Niculescu. *Delay Effects on Stability. A Robust Control Approach*. Springer, Berlin New York, 2001.

[10] T. W. Parks and C. S. Burrus. *Digital Filter Design*. Inc., New York, 1987.

[11] G. F. Franklin, J. D. Powell, and M. L. Workman. *Digital Control of Dynamic Systems*. p.151, Addison-Wesley, 1990.

[12] E. I. Jury. *Inners and Stability of Dynamic Systems*. Wiley-Interscience, New York, 1974.

[13] Th. Hélie and D. Matignon. Diffusive reprentations for the analysis and simulation of flared acoustic pipes with visco-thermal losses. *Mathematical Models and Methods in Applied Sciences*, 16:503–536, jan 2006.

[14] Th. Hélie, R. Mignot, and D. Matignon. Waveguide modeling of lossy flared acoustic pipes: Derivation of a Kelly-Lochbaum structure for real-time simulations. In *IEEE WASPAA*, pages 267–270, Mohonk, USA, 2007.